N87-22214

ESTIMATION OF SQUEEZE-FILM DAMPING AND INERTIAL COEFFICIENTS

FROM EXPERIMENTAL FREE-DECAY DATA

J.B. Roberts
University of Sussex
Brighton, England

R. Holmes
University of Southampton
Southampton, England

P.J. Mason
Chelsea College of Aeronautical and Automobile Engineering
Shoreham, Sussex, England

This paper describes the results obtained from an experimental programme concerned with a parametric identification of the damping and inertial coefficients of a cylindrical squeeze-film bearing, through an analysis of transient response data. The results enable the operating range for which a linear model of the squeeze-film is appropriate to be determined. Comparisons are made between the estimated coefficients and theoretical predictions. Presentation is by courtesy of the Council of the Institution of Mechanical Engineers, London.

INTRODUCTION

Accompanying the development of modern machinery has been an increasing demand for higher running speeds. As a result critical speeds have been encountered before the desired running speed of the machine has been reached. The consequences of this can result in failure of associated components or, in some cases, an inability to reach the desired operating speed. The present work is concerned with the squeeze-film damper, which is proving very successful in mitigating these problems. A manageable and realistic model for a squeeze-film damper can be derived by applying linearisation techniques to the oil-film forces, which are obtained by solving the Reynolds equation. This leads to a representation of the dynamic behaviour in terms of damping coefficients. The ability to provide damping is a feature of this device but there is no capacity to provide linear stiffness as the latter depends on journal rotation.

The conventional representation of a squeeze-film in terms of damping coefficients has the attraction that it is very simple to incorporate these coefficients into a discrete mathematical model of a rotor-bearing system. This approach implicitly assumes that inertial forces within the oil-film are negligible. However, theoretical investigations by a number of workers [1-11] suggest that inertial forces can be very significant in squeeze-films. Indeed, this is evident if one considers the "gap Reynolds number"

$$R_e = \frac{\rho \omega c^2}{\eta} = \frac{\text{fluid inertia force}}{\text{fluid viscous force}}$$

where ρ is the density of the lubricant, ω is the frequency of vibration, c is the radial clearance in the squeeze-film damper and η is the viscosity of the lubricant. In many practical applications R_e is of order one, or greater. For such values one cannot expect conventional lubrication theory, based on the Reynolds equation (ie. on the assumption that $R_e \ll 1$), to give an accurate representation.

In a linearised approach, inertial forces can be incorporated into the model through the introduction of "acceleration coefficients" in addition to the normal damping coefficients. However, experimental estimates of acceleration coefficients (or "hydrodynamic mass" effects), in geometries typical of many squeeze-films, do not appear in the literature; indeed, inertial effects have not been taken into account at all in many previous comparisons between theoretical and experimental dynamic behaviour. This may explain, at least partly, why it has proved so difficult to obtain satisfactory agreement between theoretical and experimental values of the damping coefficients.

In the present investigation a transient testing technique has been developed and used to obtain the dynamic characteristics of a "short" squeeze-film bearing, with a geometry typical of that currently adopted in engineering applications and with Reynolds numbers in the range $0.5 < R_e < 1.5$. The experimental results are processed using a parametric identification technique to yield estimates of the dynamic coefficients and these are compared with predictions from existing theory. Limitations of the theory are highlighted which indicate promising avenues for further research.

NOTATION

b_{rr}, b_{ss}	direct fluid damping coefficients, for the r and s directions, respectively.
$b_r{}^0, b_s{}^0$	structural damping coefficients, for the r and s directions, respectively.
B_{rr}, B_{ss}	non-dimensional, direct fluid film damping coefficients, for the r and s directions, respectively.
c	radial clearance between the journal and the bearing.
c_{rr}, c_{ss}	direct fluid film inertial coefficients, for the r and s directions, respectively.
d	initial displacement
d*	non-dimensional initial displacement (see equation (27)).
h(u)	time domain response function (see equation 17).
k_r, k_s	shaft stiffnesses, in the r and s directions, respectively.
ℓ	land length of the bearing.
m	effective, first mode mechanical mass.
m_H	hydrodynamic mass (c_{rr} in the radial direction, c_{ss} in the transverse direction).

294

P	hydrodynamic film force.
r	journal displacement in the radial direction (i.e. in the direction of the attitude line).
R	radius of the journal.
Re	Reynolds number ($=\rho\omega c^2/\eta$)
s	journal displacement in the transverse direction (i.e. in a direction perpendicular to the attitude line).
t	time.
$x(t)$	displacement.
$X(t)$	non-dimensional displacement.
$y(t)$	measured, free-decay record.
$\alpha(\omega)$	frequency response function, defined by equation (23).
$\beta(\omega)$	frequency response function, defined by equation (23).
γ	damping parameter, defined in equations (3).
γ_0	value of γ, in the absence of a fluid film.
γ^*	non-dimensionalised γ (see equations (10)).
δ	stiffness parameter, defined by equations (3).
δ_0	value of δ, in the absence of a fluid film.
δ^*	non-dimensionalised δ (see equations (10).
ζ_r, ζ_s	critical damping factors, in the case of no fluid film, in the r and s direction, respectively.
ϵ	eccentricity ratio.
ϵ_0	static eccentricity ratio.
η	absolute viscosity of the squeeze-film fluid.
ρ	density of the squeeze-film fluid.
$\Delta\tau$	sampling interval.
ω	frequency of vibration.
ω_{ro}, ω_{so}	natural frequencies of undamped vibration, in the radial and transverse directions, respectively.
τ	non-dimensional time (= $\omega_0 t$).

THEORETICAL TREATMENT

The equations of motion

The system consists of a mass of finite size (the squeeze-film journal) attached to the centre of a beam, which is built-in to rigid supports at each end and which plays the rôle of a conventional retainer spring. If the central mass is given some initial, transverse displacement, achieved by a force applied at the centre of the journal, and then released, the first mode of vibration will be dominant in the subsequent motion. Thus to a close approximation, the motion can be described in terms of two second order equations of motion.

In the present investigation, the squeeze-film bearing was run under full-film conditions, that is with no cavitation. In these circumstances, it can be shown, theoretically, that no cross-damping terms appear.

We thus write, for radial r and transverse s, displacements

$$(m + c_{rr})\ddot{r} + (b^0_r + b_{rr})\dot{r} + k_r r = 0$$
$$(m + c_{ss})\ddot{s} + (b^0_s + b_{ss})\dot{s} + k_s s = 0 \qquad \ldots (1)$$

Here c denotes inertial coefficients and b damping coefficients in the squeeze-film, b^0 denotes structural damping and k structural stiffness emanating from the spring beam. m is the effective, first mode mechanical mass. Both equations can be written in the standard form

$$\ddot{x} + \gamma\dot{x} + \delta x = 0, \qquad \ldots (2)$$

where γ and δ are constants. For the radial direction:

$$\gamma = \frac{b^0_r + b_{rr}}{m + c_{rr}}$$

$$\delta = \frac{k_r}{m + c_{rr}} \qquad \ldots (3)$$

and similarly for the transverse direction.

From a free decay test, one can determine γ and δ, by using a parametric identification technique. Suppose that a free decay test is carried out in the radial direction, in the absence of a fluid film in the squeeze-film bearing. Then $b_{rr} = c_{rr} = 0$, and we obtain the coefficients

$$\gamma_0 = \frac{b^0_r}{m} = 2\zeta_r\omega_0$$

$$\delta_0 = \frac{k_r}{m} = \omega_{ro}^2 \qquad \ldots (4)$$

where ω_{ro} is the natural frequency of undamped vibration and ζ_r is the damping factor. On combining equations (3) and (4) one obtains

$$b_{rr} = m\left[\gamma \frac{\delta_0}{\delta} - \gamma_0\right]$$

$$c_{rr} = m(\frac{\delta_0}{\delta} - 1) \qquad \ldots (5)$$

for the damping and inertial coefficients, where

$$m = \frac{k_r}{\delta_0} \qquad \ldots (6)$$

m can be determined from measurements of k_r and from a free decay test without fluid in the squeeze-film bearing (giving γ_0 and δ_0). By combining this information with estimates of γ and δ, from free decay with fluid in the squeeze-film bearing, one can estimate b_{rr} and c_{rr}, by using equation (5). Similarly, measurements of free decay in the transverse direction can be used to yield estimates of b_{ss} and c_{ss}.

In practice the structural damping is very small and one finds ω_{ro} and ω_{so} by simply measuring the frequency of vibration, without fluid in the bearing.

Before processing the decay curves it is convenient to non-dimensionalise the equation of motion (equation (2)). If ω_0 is the frequency of undamped vibration, without fluid, then a convenient non-dimensional time is

$$\tau = \omega_0 t = \delta_0^{\frac{1}{2}} t \qquad \ldots (7)$$

Also, the displacement $x(t)$, can be non-dimensionalised by dividing by the initial displacement, $x(0)$. Thus,

$$X(t) = \frac{x(t)}{x(0)} \qquad \ldots (8)$$

Equation (2) can then be recast as

$$\ddot{X} + \gamma^* \dot{X} + \delta^* X = 0 \qquad \ldots (9)$$

where

$$\gamma^* = \frac{\gamma}{\omega_0} = \frac{\gamma}{\delta_0^{\frac{1}{2}}}$$

$$\delta^* = \frac{\delta}{\omega_0^2} = \frac{\delta}{\delta_0} \qquad \ldots (10)$$

are non-dimensional coefficients and differentiation is now with respect to τ. On substituting these equations into equation (5) we obtain

$$b_{rr} = m\omega_{ro} [\gamma^*/\delta^* - \gamma_0^*] \qquad \ldots (11)$$

$$c_{rr} = m(\frac{1}{\delta^*} - 1)$$

and similarly for b_{ss} and c_{ss}.

The damping coefficients

The conventional approach to evaluating the coefficients b_{rr} and b_{ss}, for a full squeeze-film is to use the Reynolds equation as the basis of the calculation. For the general case it is necessary to solve this equation numerically, but simple, asymptotic results can be derived for

        (a) the short bearing: $\ell/R \to 0$
        (b) the long bearing: $\ell/R \to \infty$.

The short bearing theory gives the following results[12]

$$b_{rr} = \left[\frac{\pi\eta R\ell^3}{c^3} \right] \frac{(1 + 2\,\epsilon_0^2)}{(1 - \epsilon_0^2)^{5/2}}$$

$$\dots (12)$$

$$b_{ss} = \left[\frac{\pi\eta R\ell^3}{c^3} \right] \cdot \frac{1}{(1 - \epsilon_0^2)^{3/2}}$$

The corresponding long-bearing results are as follows[13]

$$b_{rr} = \left[\frac{12\pi\eta R^3\ell}{c^3} \right] \cdot \frac{1}{(1 - \epsilon_0^2)^{\frac{1}{2}}(1 - \epsilon_0^2)}$$

$$\dots (13)$$

$$b_{ss} = \left[\frac{12\pi\eta R^3\ell}{c^3} \right] \cdot \frac{2}{(2 + \epsilon_0)(1 - \epsilon_0^2)^{\frac{1}{2}}}$$

As pointed out earlier, the use of the Reynolds equation implicitly assumes that inertial forces within the fluid film are negligible. Theoretical studies of the influence of fluid inertia on the damping coefficients of a squeeze-film bearing have been undertaken by Tichy[3] and San Andrès and Vance[7]. Their results indicate that, for the particular geometry of bearing studied in this investigation, and for the range of frequencies of oscillation studied, the influence of fluid inertia on the damping coefficients is negligible.

The inertial coefficients

A linearised approach to the evaluation of squeeze-film fluid forces allows a separate evaluation of the inertial coefficients, which arise from the effect of journal acceleration.

Smith[1] has shown that for a very short full-film bearing ($\ell \ll R$) these coefficients are given by,

$$c_{rr} = \frac{\pi\rho R\ell^3}{12c} \left\{ \frac{2}{\epsilon_0^2} \left[\frac{1}{(1 - \epsilon_0^2)^{\frac{1}{2}}} - 1 \right] \right\}$$

$$\dots (14)$$

$$c_{ss} = \frac{\pi\rho R\ell^3}{12c} \left\{ \frac{2}{\epsilon_0^2} \left[1 - (1 - \epsilon_0^2)^{\frac{1}{2}} \right] \right\}$$

and $c_{rs} = c_{sr} = 0$. In the special case of zero static eccentricity ($\epsilon_0 = 0$), a limiting operation performed on equation (14) gives

$$c_{rr} = c_{ss} \quad \frac{\pi\rho R\ell^3}{12c} \quad (\epsilon_0 = 0) \qquad \dots (15)$$

This agrees with the result obtained by Fritz for very short bearings, in the concentric case[2].

For a long, full-film bearing ($\ell \gg R$) the appropriate expressions for the coefficients are as follows [1]:

$$c_{rr} = c_{ss} = \frac{\pi \rho R^3 \ell}{c} \left\{ \frac{2}{\epsilon_0{}^2} \left[1 - (1 - \epsilon_0{}^2)^{\frac{1}{2}} \right] \right\} \qquad \ldots (16)$$

and $c_{rs} = c_{sr} = 0$. In the special case where $\epsilon_0 = 0$ (concentric operation) equation (16) reduces to

$$c_{rr} = c_{ss} = \frac{\pi \rho R^3 \ell}{c} \quad (\epsilon_0 = 0) \qquad \ldots (17)$$

which is a result first derived by Stokes [14].

It is interesting to note that, for $\epsilon_0 = 0$, the ratio of c_{rr} for the long bearing case to c_{rr} for the short bearing case, is from equations (15) and (17).

$$12(\frac{R}{\ell})^2$$

The damping coefficients from the long and short bearing theories, for the concentric case, are in exactly the same ratio (see equations (12) and (13)). It follows that, for short bearings ($\ell \ll R$), the damping and inertial coefficients are, according to the short bearing theory, considerably less than those predicted from the long bearing theory.

Recently Szeri et al [9] have presented, graphically, numerical values for the inertial coefficients, c_{rr} and c_{ss}, for squeeze-films with finite values of ℓ/R, in the range $0.2 < \ell/R < 4.0$. They found it necessary to introduce an approximation, based on the assumption that ℓ/R is small, in their analysis but have indicated that their results should be more accurate than a full short-bearing approximation, provided that ℓ/R is small. Their numerical results are in virtually exact agreement with Smith's short-bearing results (equation (14)) for $\ell/R < 0.5$.

2.4 Parametric identification

It was shown in section 2.1 that the damping and inertial coefficients can be related to the non-dimensional parameters γ^* and δ^*, which occur in the second-order linear equation of motion given by equation (9). From the experiment to be described one can obtain a free-decay curve - i.e. $X(t)$ versus time. The problem is then to find, the values of γ^* and δ^* for which the solution to equation (9) gives a "best fit" to the experimental observations.

This is a problem in parametric identification, on which considerable literature exists (for example see Ref. [15]). Of the various available techniques, we have here selected the sequential method of Detchmady and Stidhar[16], since this enables estimates to be obtained from a knowledge of a single measured state variable (here the displacement of the journal versus time - either $r(t)$ or $s(t)$). Details of the algorithm are given in the Appendix.

The algorithm operates on a discretely sampled record of the decay curve. Suppose the experimental values are of $y(i\Delta\tau)$ ($i=0,1,2,\ldots$), where $\Delta\tau$ is the sampling interval and τ is given by equation (7). The data is conveniently scaled so that the start displacement $y(0)$, is unity. By sequentially processing the data, the algorithm generates least-square estimates of the state vectors $X(t)$ and $\dot{X}(t)$,

and also least-square estimates of $\gamma*$ and $\delta*$, at the times $i\Delta\tau$. These estimates "track" the experimental data and should converge as time increases - i.e. the estimated state vector $X(t)$ should approach the measured response, $y(t)$, and the estimated values of $\gamma*$ and $\delta*$ should approach constant values.

To obtain improved estimates of $\gamma*$ and $\delta*$, the algorithm can be applied in an iterative manner. In the first iteration, values of $\gamma*$ and $\delta*$ are guessed and used to start the sequential estimation computation. The algorithm will give estimates of $\gamma*$ and $\delta*$, at the end of the data sequence; i.e. at time τ_m, where τ_m is the time of the last data sample. These estimates can now be used, in place of the initial guesses, as a start to the second iteration. By repeating the iteration a number of times, the estimates of $\gamma*$ and $\delta*$, at time τ_m, should converge to constant values.

Prior to using this procedure on real decay data it was tested thoroughly on simulated data, from which it could be concluded that the algorithm was an efficient and useful method, for the present application.

Memory effects

The use of damping and inertial coefficients is based on the assumption that the fluid film forces depend only on the <u>instantaneous</u> velocity and acceleration of the journal. Although the coefficient approach is simple to incorporate into a discrete mathematical model of a rotor-bearing system, there are two serious objections which can be raised, concerning its validity:

(i)   Implicit in the method is the assumption that the velocity and accelera- tion are linearly independent variables, so far as the fluid film is concerned. This poses conceptual difficulties - e.g. how can the accel- eration be varied whilst the velocity is held constant?

(ii)   No allowance is made for "memory" effects, which can be expected when the bearing is running under cavitation conditions. Even in the case of a completely non-cavitated bearing, considered in the experimental work reported here, memory effects may be significant, for sufficiently high frequency motion, due to the visco-elastic properties of typical lubri- cants (e.g. see Ref.[3]).

Considering, for example, the case of radial motion only, a general <u>linear</u> form for the relationship between the hydrodynamic force P_r, and the motion, $\overline{r(t)}$, is as follows:

$$P_r(t) = \int_{-\infty}^{\infty} h(t - \tau) \, r(\tau) \, d\tau \qquad \ldots (18)$$

Where $h(\ )$ is a time domain impulse response function.

The use of equation (18) allows a generalisation of the coefficient representa- tion discussed earlier. To demonstrate this, consider the simple case of harmonic motion

$$r(\tau) = Ae^{i\omega\tau} \qquad \ldots (19)$$

On substituting this motion into equation (18) one obtains

$$P_r(t) = Ae^{i\omega t}[\alpha(\omega) + i\beta(\omega)] \qquad \ldots (20)$$

300

where

$$\alpha(\omega) = -\int_{-\infty}^{\infty} h(u) \cos \omega u \, du$$

$$\beta(\omega) = \int_{-\infty}^{\infty} h(u) \sin \omega u \, du$$

... (21)

Equation (20) may be compared with the corresponding result obtained by the coefficient approach, which states that, for a squeeze-film bearing

$$P_r(t) = b_{rr} \, \dot{r} + c_{rr} \, \ddot{r}$$

... (22)

Combining equations (19) and (22) one has

$$P_r(t) = A^{i\omega t} [-\omega^2 c_{rr} + i\omega b_{rr}]$$

... (23)

Equations (20) and (23) are identical if

$$\alpha(\omega) = -c_{rr} \, \omega^2$$

$$\beta(\omega) = b_{rr}\omega$$

... (24)

However, the integral representation of equation (18) allows an arbitrary variation of the "coefficients" with frequency, whereas, according to the coefficient approach, the damping and inertial coefficients are necessarily independent of frequency.

It remains to be tested by experiment whether, over a frequency range of practical concern, the frequency independent coefficient approach gives a satisfactory approximation, or whether there is a significant "memory effect", with the result that the coefficients must be treated as frequency dependent parameters. In the latter case, an integral representation, such as that given by equation (18) is more appropriate than the coefficient representation.

DESIGN OF EXPERIMENT

An outline drawing of the general arrangement of the rig is shown in Fig. 1 and a photograph of the rig is shown in Fig. 2. A non-rotating journal is contained within the circular bearing and is supported by a beam of circular cross-section which provides a stiffness in parallel with the squeeze-film. A cross-sectional view of the journal and beam assembly is shown in Fig. 3. The journal is heat shrunk along its entire contact length with the beam, and the beam is rigidly clamped at both ends. In the experimental work, three different beams were used, of varying stiffness.

Adjustment of the static equilibrium position in the horizontal direction was achieved by providing a machined channel in which the bearing housing could slide. Care was taken to ensure that the journal was accurately aligned with respect to the bearing. The alignment could be adjusted by moving the position of the beam end supports, using shims. Angular misalignment could be effectively eliminated by ensuring that the distance through which the journal could be moved, within the bearing, was maximised.

The bearing consisted of two plain lands separated by a central circumferential groove. Lubricant was supplied from a pump, through top and bottom feed holes and distributed around the bearing by the groove. No end seals were fitted and the lubricant was free to discharge into a reservoir prior to recirculation. By applying an adequate supply pressure to the inlet oil, full lubricant film conditions were maintained with no cavitation.

The experimental technique consisted of pulling back the journal, across the clearance circle, to a known position by a length of wire looped over the core of a solenoid. The journal was released by actuating the solenoid. Capacitive probes then transmitted the transient decay to a microprocessor based data-acquisition system. This allowed the dynamic characteristics (i.e. the mass, stiffness and damping of the squeeze-film, support beam and journal mass) to be evaluated and compared with simple linear theory.

EXPERIMENTAL RESULTS

In all the tests reported here the line of centres of journal and bearing, ie the radial direction, was horizontal when the journal was in its static equilibrium position. In the radial tests the journal was pulled out radially a further initial displacement, d, and released. Processing of the results from these tests enabled estimates of the damping coefficient, b_{rr}, and the inertial coefficient c_{rr}, to be derived. In the transverse tests, the journal was given an initial transverse displacement, d, (perpendicular to the line of centres) and released. From these tests, estimates of the damping coefficient, b_{ss}, and the inertial coefficient, c_{ss}, could be derived.

It is convenient, henceforth, to refer to a non-dimensional initial displacement, d*, defined by

$$d* = \frac{\text{initial displacement (d)}}{\text{radial clearance (c)}} \qquad \ldots (25)$$

Tests without fluid in the bearing

For each of the three beams available, tests were carried out, in both the radial and transverse directions, with no fluid in the squeeze-film bearing. Here the damping is very small, and is structural in origin; it follows that the measured natural frequency of oscillation is, in these circumstances, a very close approximation to the undamped natural frequency

By applying the parametric identification procedure to the results, estimates of the undamped natural frequencies, ω_0, and the structural damping factor, ζ, were obtained. For a given shaft these values were found to differ slightly, in the radial and transverse directions (the maximum difference was about 5%),and results from each direction were averaged. Table 1 summarises the results obtained from these tests.

Tests with fluid in the bearing

A series of tests was carried out, with Tellus R10 as a lubricant in the squeeze-film bearing, and with a sufficient supply pressure to ensure that full-film conditions were maintained throughout (i.e. no cavitation). Measured decay curves, in both radial and transverse directions, were obtained for static eccentricity

ratios of 0, 0.1, 0.2, 0.3, 0.4 and 0.5 and for initial displacements, d*, of 0.2 and 0.4. The decay curves were normalised, in every case, to give an initial displacement of unity.

If the journal-bearing system behaves linearly, then the normalised decay curves should be independent of the initial displacement, d*, if other parameters are kept constant. Thus by performing a series of decay tests, with differing initial displacements, and comparing normalised decay curves, one can assess the range within the bearing clearance circle, for which linear conditions prevail.

At ϵ_0 = 0.0 and ϵ_0 = 0.3, the system behaved linearly (to a close approximation), in both directions, for start amplitudes up to d* = 0.4. At the highest static eccentricity ratio studied, ϵ_0 = 0.5, a good collapse of the normalised decay curves was still obtained in the transverse direction for d* = 0.2 and 0.4, whereas, in the radial direction there was distinct evidence of non-linearity, for d* = 0.4. It can be concluded that there is a fairly wide range of journal displacement position, within the clearance circle, for which a linear mathematical representation is reasonable.

Figs. 4 (a) to (f) show a set of experimental, normalised decay curves, obtained with the squeeze-film journal mounted on beam 1. The results cover the static eccentricity range ϵ_0 = 0.0 to 0.5, and relate to both radial and transverse tests. Similar series of results were obtained for beams 2 and 3. In general, for each beam, ϵ_0 value, and chosen direction, results were obtained for d* = 0.2 and 0.4; where these collapsed reasonably well they were averaged to produce curves such as those shown in Fig. 5. Where non-linearity was indicated by a lack of collapse (generally at ϵ_0 = 0.4 and ϵ_0 = 0.5, in the radial direction), the result for d* = 0.2 only was used.

A comparison between the results for ϵ_0 = 0.0 for beam 1, in the radial and transverse directions, (see Figs. 5(a) and (b)) indicates some degree of asymmetry in the journal bearing configuration. For example, the second, positive overshoot in the radial direction is appreciably less than that observed in the transverse direction. The reason for this asymmetry is not clear, but may be due to the geometry of the oil-feed arrangement (fluid was supplied at the top and bottom of the central circumferential groove). The corresponding results for beams 2 and 3 indicated that the asymmetry was much less marked at higher frequencies of oscillation.

Beam stiffness results

To enable estimates of the damping and inertial coefficients to be derived from the free decay data, it is necessary to know the value of the effective, first mode mass, m. This value will be related to the actual mass of the journal, together with the mass of the beam, and so will vary, depending upon which beam is used in the experiments.

In the face of various uncertainties regarding the precise end conditions of the beams, it was decided to evaluate m, for each beam, from a knowledge of the natural frequency of oscillation, ω_0, and the beam stiffness. Thus

$$m = \frac{k}{\omega_0{}^2}$$

will give an estimate of m, if k is the effective, first mode stiffness.

303

The beam stiffness, k, was determined experimentally, by pulling the journal, radially, with a known static force, and measuring the resulting radial journal displacement. Table 1 shows the results obtained for the effective masses of the journal and beams.

COMPARISON BETWEEN THEORY AND EXPERIMENT

Parameter estimation

As a first stage in the analysis of the decay data, the parameter estimation procedure described in section 2 was applied to each decay curve. This yielded estimates of the parameters γ^* and δ^*, in the linear, second order model given by equation (9).

Figs. 6 show typical results of applying the estimation method to a particular decay curve. Here the experimental decay curve of Fig 6(b) was obtained for beam 1, in the radial direction, and with the journal initially concentric ($\varepsilon_0 = 0$) (see also Fig. 5(a)). The iterative technique, described in section 2, was used to refine the estimates of γ^* and δ^*, denoted $\hat{\gamma}^*$ and $\hat{\delta}^*$, respectively. Fig. 6(a) shows the variation of $\hat{\gamma}^*$ and $\hat{\delta}^*$, with time (measured in units of $\tau = \omega_0 t$) during the fifth iteration; at this iteration stage convergence is achieved, as evidenced by the fact that the final estimates in the cycle are equal to the initial estimates ($\hat{\gamma}^* = 0.601$, $\hat{\delta}^* = 0.662$). Fig.6(b) shows a corresponding comparison (for the fifth iteration, again) between the estimated displacement state variable, $\hat{X}(t)$, and the experimental decay curve; this shows that the estimated state "tracks" the experimental curve extremely well. A better idea of the degree of fit achieved can be obtained by comparing the experimental curve with the theoretical curve, found by using the final parameter estimates; this comparison is shown in Fig. 6(c).

The excellent degree of fit obtained in Fig. 6(c) can only be obtained, of course, by allowing both the parameters γ^* and δ^* to "float". If one assumes that the squeeze-film produces only a damping effect then it is necessary to set $\delta^* = 1$ and to obtain a best fit by allowing only γ^* to vary. This can be achieved, using the same parametric identification procedure as before, but setting the initial, off-diagonal elements of the P matrix to zero (see Appendix); this has the effect of "locking" the δ^* parameter to its initially set value, with the result that optimisation is sought with respect to the γ^* parameter alone. Fig. 6(d) shows a comparison between the experimental decay curve and the best-fit theoretical curve, with $\delta^* = 1.0$ and γ^* optimised ($\gamma^* = 0.912$). A comparison between Figs. 6(c) and (d) reveals that the effect of deviations of δ^* from unity (due to inertial effects in the squeeze-film) is very significant and that a very poor fit to the data is achieved by assuming that only damping is present in the squeeze-film. Similar comparisons have been made with other decay curves and these lead to a similar conclusion.

Damping and inertial coefficients

Once γ^* and δ^* have been estimated from a particular decay curve, then the damping and inertial coefficients may be found.

To present the damping results it is convenient to introduce the non-dimensional coefficients per land.

$$B_{rr} = b_{rr} \frac{c^3}{2\pi\eta R\ell^3}$$

$$B_{ss} = b_{ss} \frac{c^3}{2\pi\eta R\ell^3}$$

... (26)

According to the short-bearing theory,(equation (12)),

$$B_{rr} = \frac{(1 + 2\epsilon_0^2)}{(1 - \epsilon_0^2)^{5/2}}$$

and

... (27)

$$B_{ss} = \frac{1}{(1 - \epsilon_0^2)^{3/2}}$$

In the experimental rig the following values apply:

$R = 0.06$ m, $c = 2.54 \times 10^{-4}$m, $\ell = 0.012$ m, $\eta = 22 \times 10^{-3}$ Ns/m^2,

Using these values in equations (26), and equations (11) one obtains an equation for B_{rr} (and also B_{ss}) of the form

$$B_{rr} = k_i \frac{\gamma^*_{cor}}{\delta^*} \quad (i = 1,2,3)$$

... (28)

where

$$\gamma^*_{cor} = \gamma^* - \gamma_0^* \delta^*$$

... (29)

is the damping parameter, corrected for the effect of structural damping and k_i is a non-dimensional constant, dependent on the beam used. The appropriate k_i values are given in Table 1

The relationship between the present experimental values of B_{rr} and B_{ss}, and the corresponding theoretical values, according to both long and short-bearing theories, is shown in Figs. 7(a) and (b). It is evident that the experimental values lie much closer to the short-bearing theoretical curve. At zero eccentricity there is a factor of 300 between the two theoretical values, whereas the experimental values are only a factor of about 1.5 higher than the short-bearing theoretical result. There is little indication of any "memory effect", due to changes in the natural frequency of oscillation.

The inertial coefficients, c_{rr} and c_{ss}, defined in section 2, have the physical significance of hydrodynamic masses. Thus m_H, the hydrodynamic mass, is given by

$$m_H = c_{rr} \text{ (radially)}$$

$$= c_{ss} \text{ (transversely)}$$

Figs. 8(a) and (b) show the variations of m_H with static eccentricity ratio, ϵ_0, for the radial and transverse directions, respectively. Here the experimental estimates of m_H are compared with both long and short bearing theoretical values. The significant feature here is the magnitude of the inertial effect. In both directions, the hydrodynamic mass is an order of magnitude greater than the short bearing theoretical prediction. This is rather surprising in view of the small ℓ/R ratio pertaining in the experimental rig (0.2). For this value of ℓ/R the results of Szeri et al[9] lead one to expect that the short-bearing theory should give a reasonably accurate estimate of m_H.

305

CONCLUSIONS

Damping coefficients for both the radial and transverse directions, agreed reasonably well with the short-bearing theoretical results, although the experimental values were generally higher than the theoretical values. The variation of damping coefficients with static eccentricity ratio, ε_0, was very similar to the variation predicted by short-bearing theory. Thus, in the radial direction there was a marked increase in damping coefficient with ε_0, whereas in the transverse direction this effect was much less significant.

The experimentally-determined inertial coefficients (or hydrodynamic masses) were generally much higher than the theoretical values given by the short-bearing theory - typically an order of magnitude higher.

The experimentally determined damping and inertial coefficients, for the three shafts, were found to collapse fairly well, when plotted against static eccentricity ratio. This is a strong indication that, at least over the frequency range studied here, "memory effects" within the squeeze film are not significant.

APPENDIX

Parametric Identification of Free Decay Data

General theory

Consider a dynamic system defined by the following differential equation of motion:

$$\dot{\underset{\sim}{x}} = \underset{\sim}{g}(\underset{\sim}{x}) \qquad \ldots (A1)$$

Here x is an n-vector containing the states, x_1, x_2, ...,x_n, of the system and $g(x)$ is an n-vector function. If the system is stable, and is released from some initial condition, $x(0)$, then a transient response will result, with the motion decaying to zero. Suppose that observations of the output, or response, of the system are made during the time interval $0 < t < T$. An observation vector, $y(t)$ will be defined by

$$\underset{\sim}{y}(t) = \underset{\sim}{h}(\underset{\sim}{x}) + (\text{observation error}) \qquad \ldots (A2)$$

where y is an m-vector output and h is an m-vector function. Here the (observation error) term accounts for the fact that the output observation is of limited precision, due to quantisation errors in A/D conversion, electrical noise, etc. The estimation problem is to estimate the state vector $x(T)$ from the observation vector $y(t)$, measured in the interval $0 < t < T$ - i.e. to find the vector $\hat{x}(T)$, say, which corresponds to a "best fit" to the observations, and is consistent with equation (A1).

A "best fit" is most conveniently achieved in a least-square sense. Suppose that the following residual errors are defined:

$$\underset{\sim}{\varepsilon_1}(t) = \underset{\sim}{y}(t) - \underset{\sim}{h}(\underset{\sim}{x}^*) \qquad \ldots (A3)$$

$$\underset{\sim}{\varepsilon_2}(t) = \dot{\underset{\sim}{x}}^* - \underset{\sim}{g}(\underset{\sim}{x}^*) \qquad \ldots (A4)$$

Here x* is a "nominal" trajectory - i.e. a possible time history of x. From the residual errors one can form the integral

$$I = \int_0^T [\,||\underset{\sim}{\epsilon_1}(t)||_{Q^2} + ||\underset{\sim}{\epsilon_2}(t)||_{W^2}\,]dt \qquad \ldots (A5)$$

where $||\cdot||_{Q^2}$ and $||\cdot||_{W^2}$ are suitably defined quasi-norms.

Suppose that I is minimised when $x^*(t) = \hat{\underset{\sim}{x}}(t)$; a least-squares estimate of x(T) is then $\hat{\underset{\sim}{x}}(T)$.

In practice, y(t) is usually measured at equi-spaced times, $t_i \times i\Delta t$ (i = 0,1,2,...). It is then convenient to use a recursive algorithm, which will generate sequential estimates of $\hat{\underset{\sim}{x}}(t)$, at times t_i. It has been shown by Detchmendy and Stidhar[16], using the method of invariant imbedding, that $\hat{\underset{\sim}{x}}(t)$ can be generated sequentially by using the following equations:

$$\frac{d\hat{\underset{\sim}{x}}}{dt} = \underset{\sim}{g}(\hat{\underset{\sim}{x}}) + 2\underset{\sim}{P}(t)\ \underset{\sim}{H}(\hat{\underset{\sim}{x}})\ \underset{\sim}{Q}\{y(t) - \underset{\sim}{h}(\hat{\underset{\sim}{x}})\} \qquad \ldots (A6)$$

$$\frac{d\underset{\sim}{P}}{dt} = \frac{\partial \underset{\sim}{g}}{\partial \hat{\underset{\sim}{x}}}\ \underset{\sim}{P} + \underset{\sim}{P}\left[\frac{\partial \underset{\sim}{g}}{\partial \hat{\underset{\sim}{x}}}\right]^T + 2\underset{\sim}{P}\ \frac{\partial}{\partial \hat{\underset{\sim}{x}}}\ [\underset{\sim}{H}(\hat{\underset{\sim}{x}})\underset{\sim}{Q}\{y(t) - \underset{\sim}{h}(\hat{\underset{\sim}{x}})\}]\underset{\sim}{P} \qquad \ldots (A7)$$

where

$$\underset{\sim}{H}(\hat{\underset{\sim}{x}}) = \left|\frac{\partial}{\partial \hat{\underset{\sim}{x}}}\ \underset{\sim}{h}(\hat{\underset{\sim}{x}})\right|^T \qquad \ldots (A8)$$

Here P(t) is an n x n matrix and Q is an m x m matrix. The latter matrix allows weighting to be assigned to the elements in the observation vector. H is an n x m matrix.

By integration of equations (A6) and (A7) one can generate estimates, $\hat{\underset{\sim}{x}}(t_i)$, at the observation times, t_i. An initial estimate, $\hat{\underset{\sim}{x}}(0)$ of the start condition, $\underset{\sim}{x}(o)$, is required, but the estimates $\hat{\underset{\sim}{x}}(T)$ will usually be insensitive to the choice of $\hat{\underset{\sim}{x}}(0)$, providing that T is sufficiently large.

REFERENCES

1. Smith, D.M. "Journal Bearing Dynamic Characteristics - Effect of Inertia of Lubricant", Proc. Inst. Mech.Engs., Vol.179, Part 3J, 1964-65, pp.37-44.

2. Fritz, R.J. "The Effects of an Annual Fluid on the Vibrations of a Cory Rotor. Part 2 - 1st", Trans. ASME, Journal of Basic Engineering, Vol. 20, 1970, pp.930-937.

3. Tichy, J.A. "Effects of Fluid Inertia and Visco-elasticity on Squeeze-Film Bearing Forces", ASLE Trans., Vol.25, Part 1, January 1982, pp.125-132.

4. Tichy, J.A. "Effects of Fluid Inertia and Viscoelasticity on Forces in the Infinite Squeeze-Film Bearing", ASLE Paper 83-AM-3E-1, 1983.

5. Tichy, J.A. "The Effect of Fluid Inertia in Squeeze-Film Damper Bearings : A Heuristic and Physical Description", ASME Paper No. 83-GT-177, 1983.

6. Tichy, J.A. "Measurement of Squeeze-Film Bearing Forces to Demonstrate the Effect of Fluid Inertia", ASME Paper No. 84-GT-11, 1984.

7. San Andrés, L. and Vance, J.M. "Effects of Fluid Inertia and Turbulence on Force Coefficients for Squeeze-Film Dampers", NASA publication CP 2338 (1984).

8. Reinhardt, E. and Lund, J.W. "The Influence of Fluid Inertia on the Dynamic Properties of Journal Bearings", Journal of Lubrication Technology, ASME, Vol. 97, 1975, pp.159-175.

9. Szeri, A.Z., Raimondi, A.A. and Giran-Duarte, A. "Linear Force Coefficients for Squeeze-Film Dampers", Journal of Lubrication Technology, ASME, Vol. 195, 1983, pp.326-334.

10. Lund, J.W. Smalley, A.J., Tecza, J.A. and Walton, J.F., "Squeeze Film Damper Technology : Part 1 - Prediction of Finite Length Damper Performance, ASME PAPER 83-GT-247, 1983.

11. Nelson, C. "The Effect of Turbulence and Fluid Inertia on a Squeeze-film Damper", AlAA/SAE/ASME 16th Joint Propulsion Conference, June 30-July 2, 1980.

12. Holmes, R. "The Vibration of a Rigid Shaft on Short Sleeve Bearings", J.Mech.Eng. Science, Vol. 2, 1960, pp 337-341.

13. Holmes, R. "Oil-Whirl Characteristics of a Rigid Rotor in 360° Journal Bearings", Proc. Inst. Mech. Engs., Vol.117, No. 11, 1963, pp.291-308.

14. Stokes, G.G. "On Some Cases of Fluid Motion", Proceedings of the Cambridge Philosophical Society, Vol. 8, May 1843, pp.105-137.

15. Astrom, K.J. and Eykhoff, P. "System Identification - a Survey", Automatica, Vol. 7, 1971, pp123-162.

16. Detchmendy, D.M. and Stridhar, R. "Sequential Estimation of States and Parameters in Noisy Non-linear Dynamical Systems", Trans. ASME, Journal of Basic Engineering, Vol.16, 1966, pp.363-368.

TABLE 1

Beam No.	Nat. freq. (Hz)	Damping factor $\zeta = \gamma_0^*/2$	Effective mass of journal & beam (kg)	k_i
1	33.8	0.010	7.73	1.88
2	58.8	0.010	8.35	3.53
3	94.3	0.015	9.60	6.50
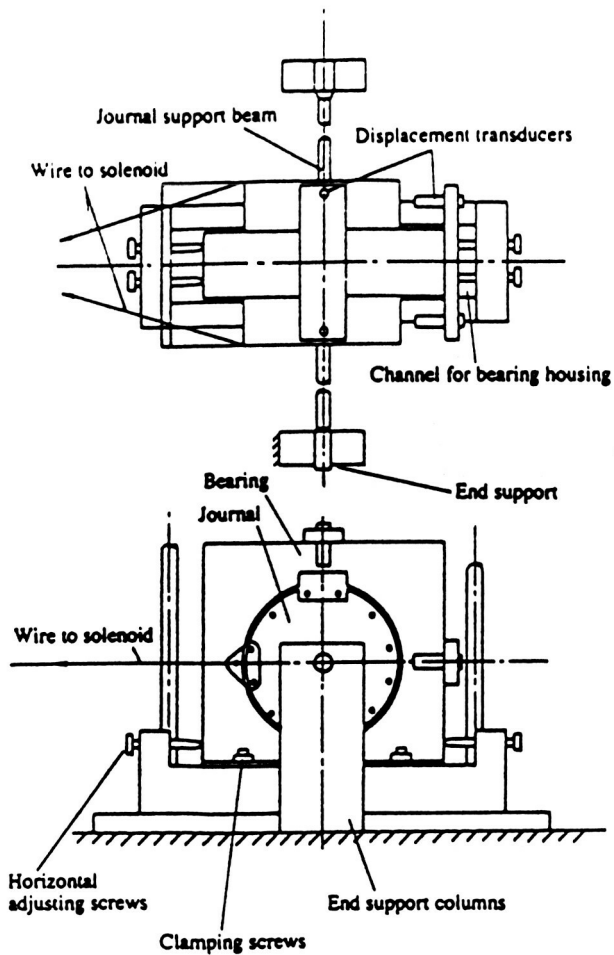
Figure 1. – Squeeze-film bearing rig.
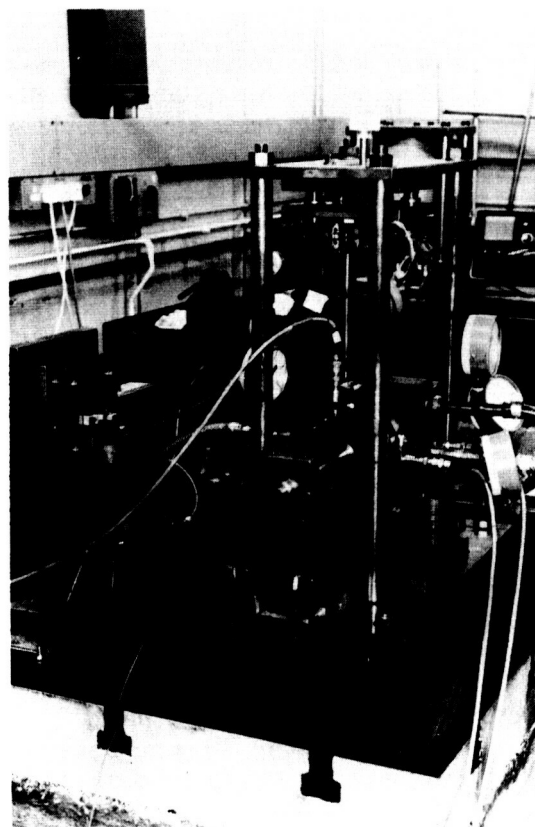
Figure 2. – Photograph of the experimental rig.
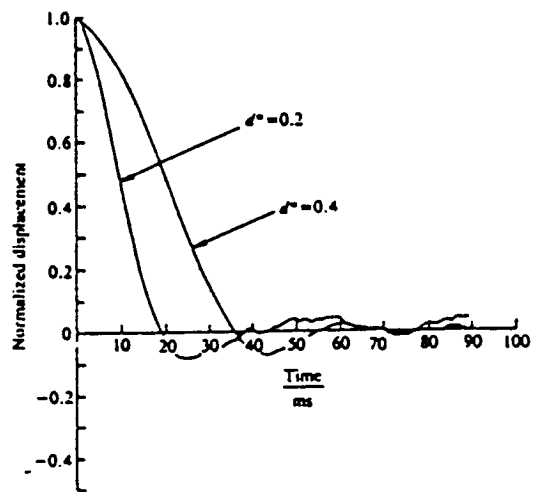
309
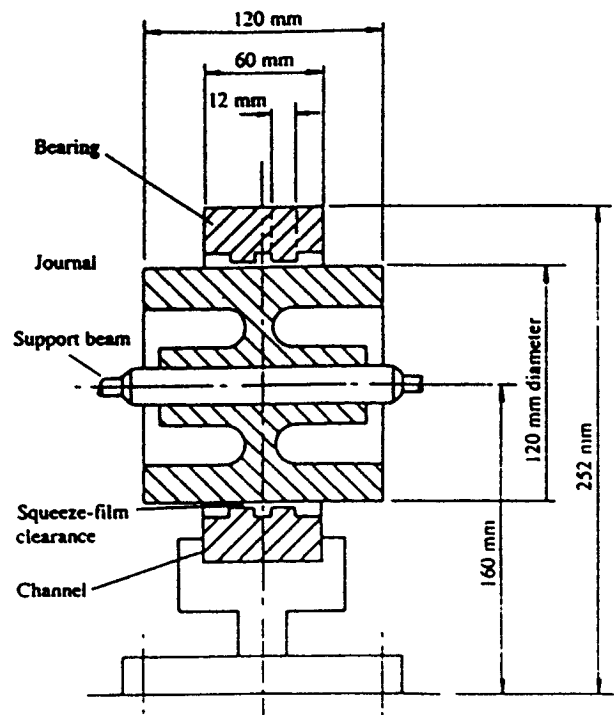
Figure 3. - Cross section of journal
and beam assembly.

(a) $\epsilon_O = 0$; radial displacement.
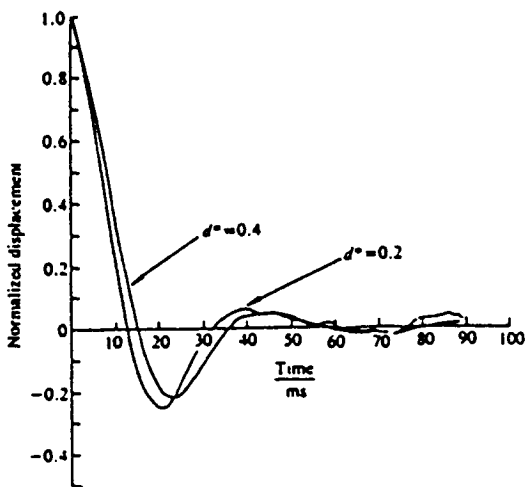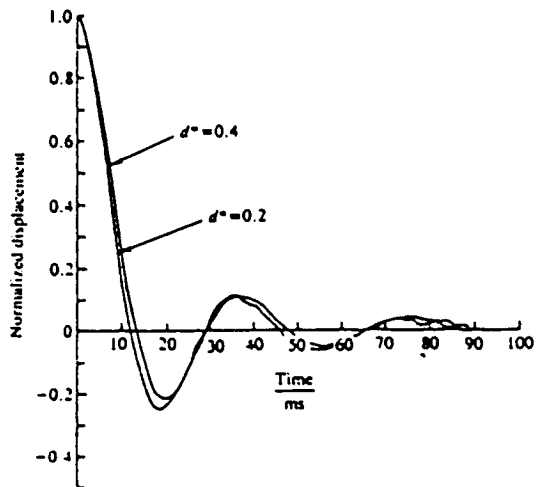
(b) $\epsilon_O = 0$; transverse displacement.
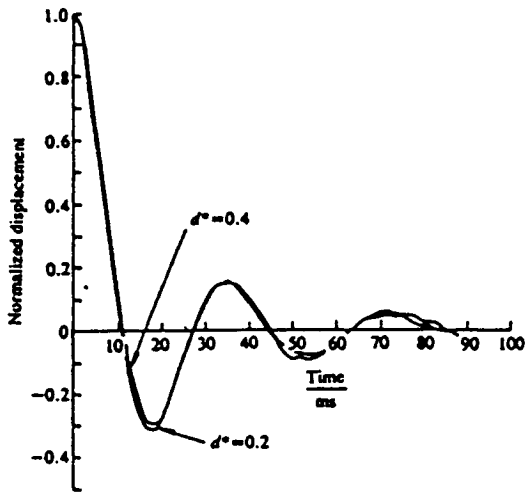
(c) $\epsilon_O = 0.3$; radial displacement.

(d) $\epsilon_O = 0.3$; transverse displacement.
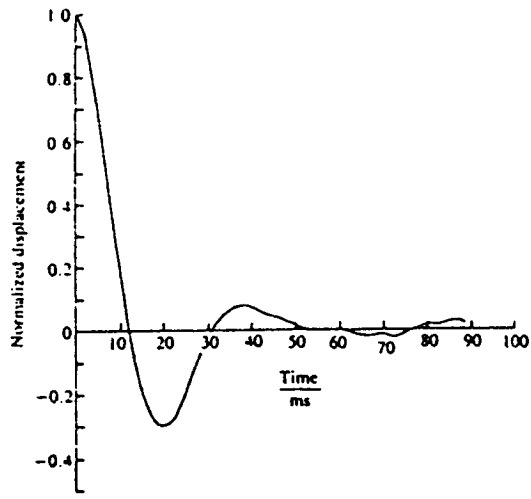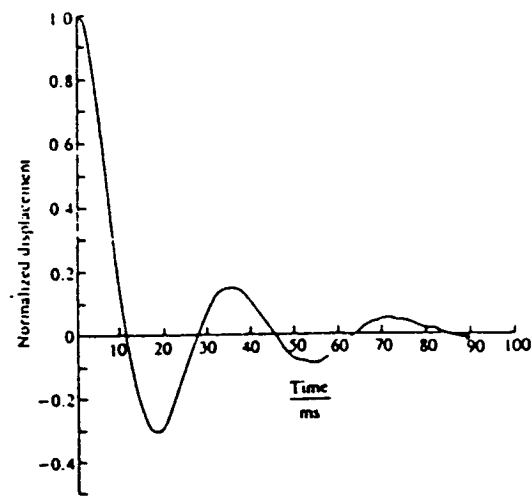
(e) $\epsilon_O = 0.5$; radial displacement.

(f) $\epsilon_O = 0.5$; transverse displacement.
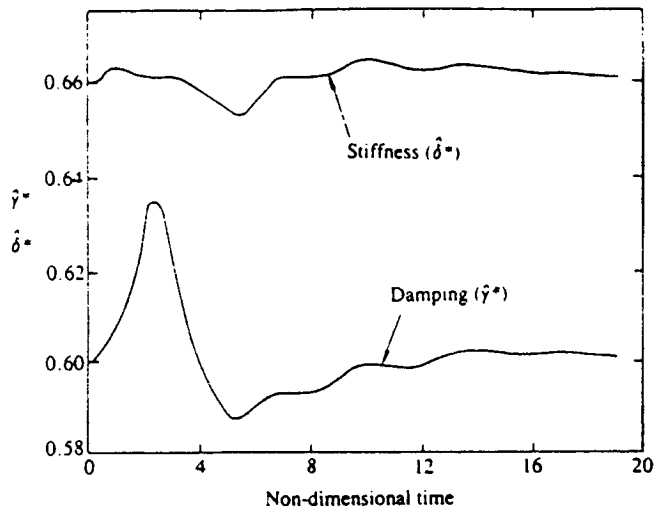
Figure 4. - Experimental transient decay results; beam 1.

(a) $\epsilon_0 = 0$; radial displacement.

(b) $\epsilon_0 = 0$; transverse displacement.

Figure 5. – Averaged experimental transient decay results.

(a) Variation of $\hat{\delta}*$ and $\hat{\gamma}*$ with non-dimensional time.
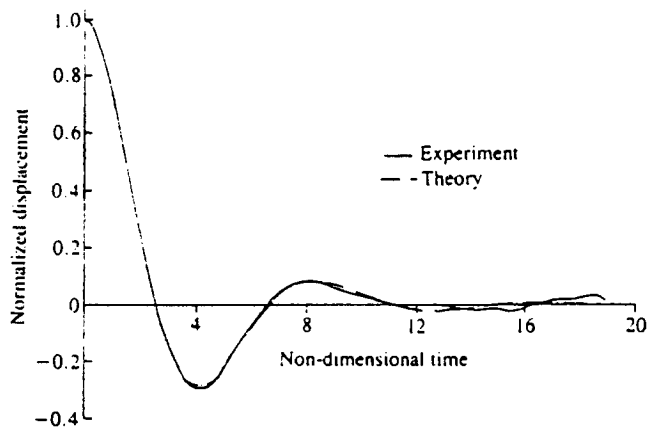
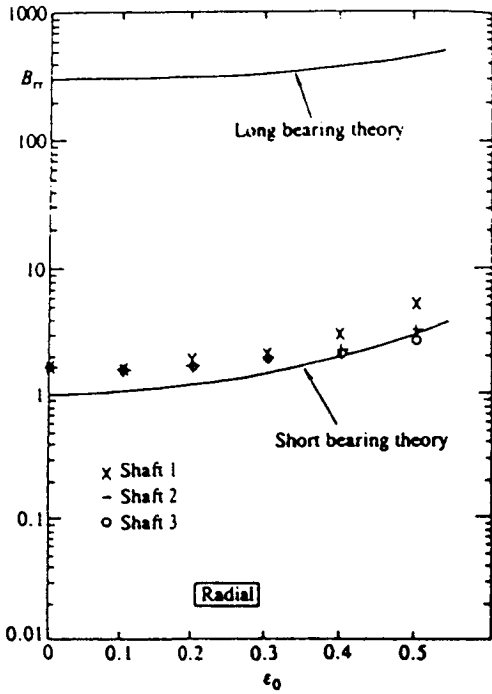(c) Comparison between the experimental decay curve and the theoretical curve, using final parameter estimates.
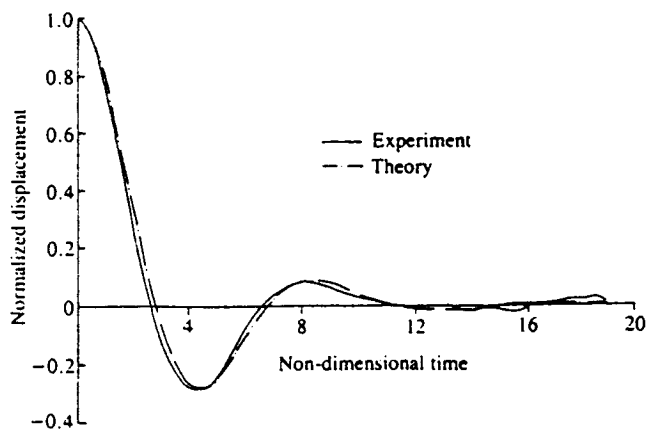
(b) Comparison between the experimental decay curve and the estimated displacement state variable, $\hat{X}(t)$.
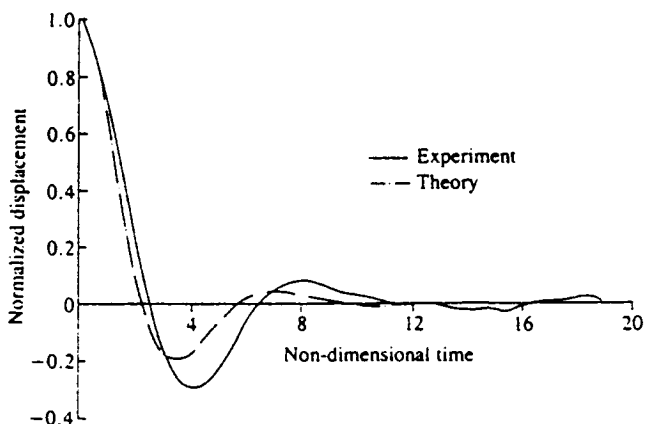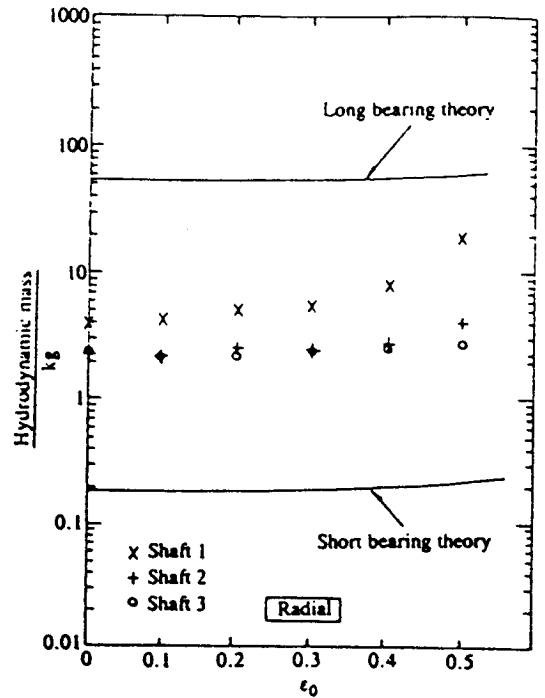
(d) Comparison between the experimental decay curve and the theoretical curve, obtained by setting $\delta* = 1$ and using the estimated value of $\gamma*$.
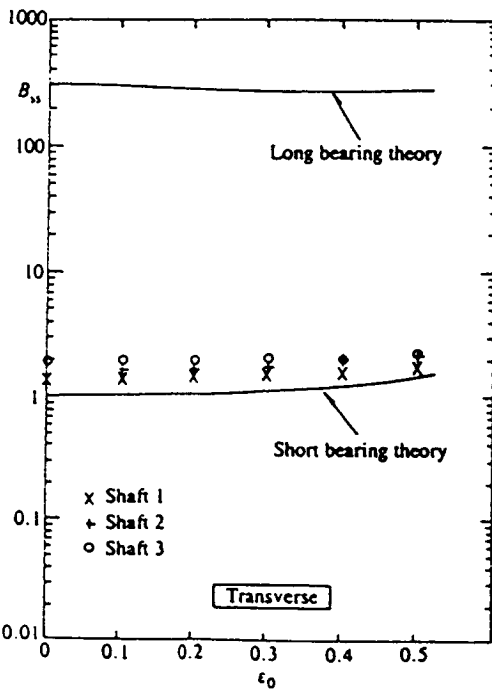
Figure 6. - Results of applying parametric identification to an averaged experimental transient decay result for $\epsilon_o = 0$; radial displacement.
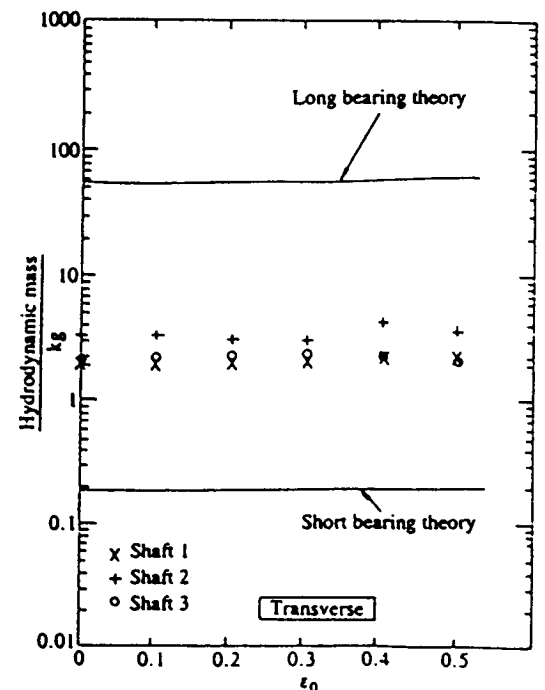
(a) B_{rr}; radial displacement.

(a) c_{rr}; radial displacement.

(b) B_{ss}; transverse displacement.

(b) c_{ss}; transverse displacement.

Figure 7. – Comparison between experimental results for B_{rr} and B_{ss} and the corresponding theoretical values, from short and long bearing theory.

Figure 8. – Comparison between experimental results for m_H and the corresponding theoretical values from short and long bearing theory.

314